Photonic-bandgap microcavities in optical waveguides

J. S. Foresi*, P. R. Villeneuve†, J. Ferrera‡, E. R. Thoen‡, G. Steinmeyer‡, S. Fan†, J. D. Joannopoulos†, L. C. Kimerling*, Henry I. Smith‡ & E. P. Ippen†‡

** Department of Materials Science and Engineering, Massachusetts Institute of Technology, Cambridge, Massachusetts 02139, USA*

† Department of Physics, Massachusetts Institute of Technology, Cambridge, Massachusetts 02139, USA

‡ Department of Electrical Engineering and Computer Science, Massachusetts Institute of Technology, Cambridge, Massachusetts 02139, USA

Confinement of light to small volumes has important implications for optical emission properties: it changes the probability of spontaneous emission from atoms, allowing both enhancement and inhibition. In photonic-bandgap (PBG) materials[1–4] (also known as photonic crystals), light can be confined within a volume of the order of $(\lambda/2n)^3$, where λ is the emission wavelength and n the refractive index of the material, by scattering from a periodic array of scattering centres. Until recently[5,6], the properties of two- and three-dimensional PBG structures have been measured only at microwave frequencies. Because the optical bandgap scales with the period of the scattering centres, feature sizes of around 100 nm are needed for manipulation of light at the infrared wavelength (1.54 μm) used for optical communications. Fabricating features this small requires the use of electron-beam or X-ray lithography. Here we report measurements of microcavity resonances in PBG structures integrated directly into a submicrometre-scale silicon waveguide. The microcavity has a resonance at a wavelength of 1.56 μm, a quality factor of 265 and a modal volume of 0.055 μm^3. This level of integration might lead to new photonic chip architectures and devices, such as zero-threshold microlasers, filters and signal routers.

A single mode waveguide is used to both confine light in the PBG structure and control the polarization of the light. A diagram of the waveguide structure is shown in Fig. 1a. The waveguide consists of a silicon (Si) strip on a silicon dioxide (SiO_2) layer. The low-index SiO_2 layer separates the guided mode from the underlying Si substrate and allows strong field confinement in the Si waveguide. The introduction of a periodic array of holes into the waveguide limits the wavevector to π/a, where a is the spatial period, or lattice constant, of the array of holes. This allowable range of wavevectors is similar to the Brillouin zone used in solid-state physics. As well as putting a limit on the wavevector, the periodic array of holes (that is, the PBG structure) has the effect of folding the dispersion relation of the strip waveguide and of splitting the lowest-order mode to form two allowable guided modes[7]. The splitting at the Brillouin zone edge is called a bandgap; its size is determined by the dielectric contrast of the periodic structure. For the device shown in Fig. 1a, the dielectric contrast is defined by the Si waveguide ($\epsilon_{Si} = 12.1$) and the air holes ($\epsilon_{air} = 1$) etched into the waveguide. The large contrast opens a gap that is 27% of the midgap frequency. With a midgap wavelength of $\lambda = 1.54\,\mu m$, the gap is 400 nm in width. This gap is significantly larger than that which can be achieved with surface-corrugated waveguides.

If a defect is included in the PBG structure, a state can be formed in the gap. This state is analogous to a defect or impurity state in a semiconductor that forms a level within the semiconductor bandgap. Defects in PBG structures are engineered by incorporating breaks in the periodicity of the PBG device. A break in periodicity leads to a defect state that is localized in real space and therefore extended in wavevector space. Controlling the coupling of this extended state to radiation modes is necessary to optimize the performance of the defect as a resonator or filter. Taking these considerations into account, we designed a PBG microcavity for operation near $\lambda = 1.54\,\mu m$. The dimensions of the device, and the computed transmission through the device, are shown in Fig. 1a, b. The computation shows a wide stop-band from 1,300 to 1,700 nm. The resonance is predicted to have a wavelength of 1,547 nm and a cavity quality factor Q of 280. The Q of the cavity is defined as $\lambda/\Delta\lambda$ of the cavity resonance and is a measure of the ratio of the optical energy stored in the microcavity to the cycle-average power radiated out of the cavity. The resonant mode is strongly confined within the microcavity. The modal volume, V, is defined as

$$VP_{max} = \int P(r)\,d^3r \qquad (1)$$

where $P(r)$ is the total electromagnetic energy density of the mode, and P_{max} is the peak value of $P(r)$. With this definition, a modal volume of 0.055 μm^3 is computed.

The minimum feature size associated with the waveguide microcavity occurs between the edges of the holes and the edge of the waveguide. For the device shown in Fig. 1a, the minimum feature size is 0.13 μm, which is currently beyond the limits of optical lithography. To achieve pattern transfer at this length scale, we used X-ray lithography with a Cu_L source at 1.3 nm; the mask was made by electron-beam lithography[8]. This approach easily resolved the 0.13 μm PBG feature. A scanning electron micrograph of a processed device is shown in Fig. 2. This device was fabricated from a Unibond silicon-on-insulator substrate with a 0.2 μm single-crystal Si layer on a 1.0 μm SiO_2 layer.

For testing purposes, we designed the waveguide to be curved at both the input and output ports. This curvature allows the input and output of the waveguide to be offset during the testing. Any light that couples through the substrate is spatially separated from the waveguide mode. Flares at both the input and output widen the guide to 5.0 μm to improve coupling into the waveguide. Total waveguide lengths of 1.5 mm were used.

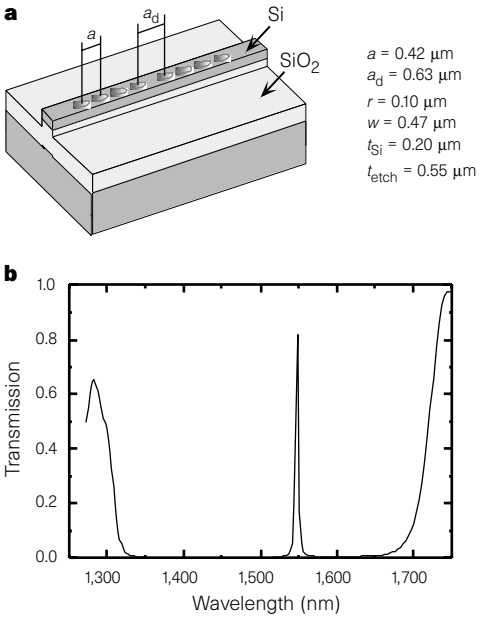

Figure 1 Dimensions and basic properties of a PBG waveguide microcavity. **a**, Schematic of a PBG waveguide microcavity with dimensions for operation at $\lambda = 1.54\,\mu m$: a is the hole period, a_d is the defect length, r is the hole radius, w is the waveguide width, t_{Si} is the silicon thickness and t_{etch} is the total etch depth through both the Si and SiO_2. **b**, Computation of the transmission through the structure. The transmission spectrum corresponds to the device dimensions listed. The resonance is centred at 1,547 nm and has a Q of 280.

To test the devices, a continuous-wave colour-centre laser ($NaCl:OH^-$) with a tuneable range from 1,500 to 1,625 nm is used. This laser has ~250 mW of output power across the tuning range. An optical multichannel analyser provides continuous monitoring of the wavelength during the testing, and a portion of the beam is split off to monitor the laser power. The laser beam is focused into an optical fibre that has a lensed output tip positioned to couple light into the waveguide. A ×40 objective lens collects the transmitted light at the waveguide output. A polarizing beam splitter allows discrimination between TE and TM polarized light. The ×40 objective images the waveguide output through the beam splitter onto a 100 μm pinhole. This pinhole reduces the amount of substrate-coupled light that reaches the detector. The wavelength reference, power monitor and transmitted power are all collected simultaneously by a data-acquisition system.

The measured transmission spectrum for a PBG waveguide microcavity with four holes on each side of the defect is shown as the solid line in Fig. 3; the theoretical transmission for this particular device is shown as a dotted line. At resonance, a sharp peak in transmission is seen. The measured Q of this resonance is 265, compared with the calculated Q of 280. This resonance wavelength is 1,560 nm, a 1% shift from the calculated resonance of 1,547 nm. The measured values are in remarkable agreement with theory. The transmission spectrum was calculated from dimensions measured on the actual device. The discrepancy between calculated and measured transmission features is well within the accuracy of the scanning electron microscopy technique used to determine the device dimensions. As mentioned earlier, the modal volume is 0.055 μm^3. This is the most spatially localized resonant photon state ever achieved and corresponds to a volume of only five times $(\lambda/2n)^3$.

Because the tuning range of the colour-centre laser is smaller than the PBG stop-band, not all of the PBG features (resonance and band edges) could be measured on a single waveguide microcavity. However, the scaleability of the PBG properties with wavelength allows tuning of the device dimensions to move the desired transmission features into the laser tuning range. We used this property to design devices with band edges within the tuning range. To see the high-frequency band edge we increased all of the dimensions, and to see the low-frequency band edge we decreased all of the dimensions. The scaling essentially shifts the transmission spectrum of Fig. 1b to longer or shorter wavelengths, but the overall shape of the spectrum does not change. It should be noted that, because all of the microcavities are processed on the same substrate, the Si thickness of the band-edge devices could not be tuned with the other dimensions.

To map all of the data onto a single plot, we performed transmission simulations using the measured dimensions of the band-edge device. The theoretical shifts were calculated and applied to the measured data. The computations take into account the deviation of the device thickness from perfect scaling, and show that the thickness variation results only in a modification of the wavelength shift, not a change in the shape of the transmission characteristic. For the upper-frequency band edge (that is, short wavelength) a shift of −194 nm was determined, and for the lower-frequency band edge a shift of +126 nm was found. The scaled data are shown in Fig. 3. Excellent agreement between theory and experiment is seen. The upper band edge is red-shifted by 1%, and the lower band edge overlaps the prediction almost exactly. Simulations indicate that the low-frequency band edge does not shift appreciably with dimensional variations, whereas the resonance and high-frequency band edges are more sensitive to changes in dimension. The transmission measurements marked the first complete evaluation of PBG guided mode properties, including resonant states, at optical frequencies.

The resonance wavelength of the PBG waveguide microcavity can be altered by changing the size of the defect[3]. The results shown in Figs 1–3 were obtained with a defect length a_d of 1.50a, where a is the period of the PBG holes. In Fig. 4 we show measured resonances

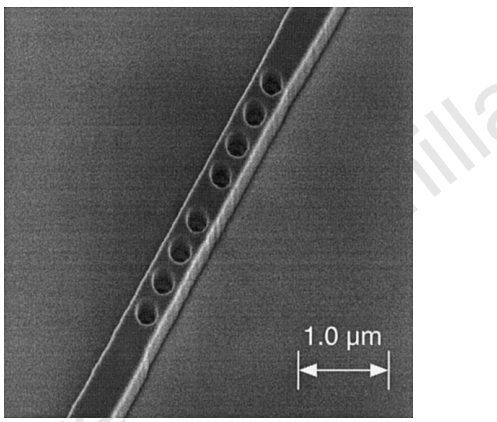

Figure 2 Scanning electron micrograph of a PBG waveguide microcavity fabricated by X-ray lithography. The pattern was transferred to the Unibond silicon-on-insulator substrate with a Cr lift-off mask. The Si etching was performed in a plasma of CF_4 and O_2; the SiO_2 etching used a CHF_3 plasma. After etching, the Cr was removed and the samples were cut and polished for testing.

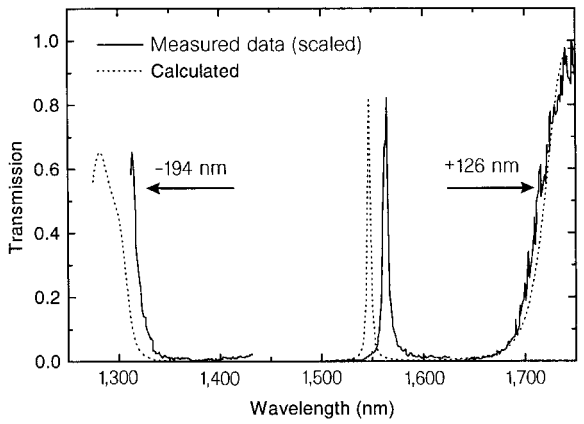

Figure 3 Comparison of measured transmission (solid lines) to calculated transmission (dotted line) for a PBG microcavity with four holes on each side of the microcavity. The upper-band and lower-band edge transmission data have been shifted in wavelength as described in the text.

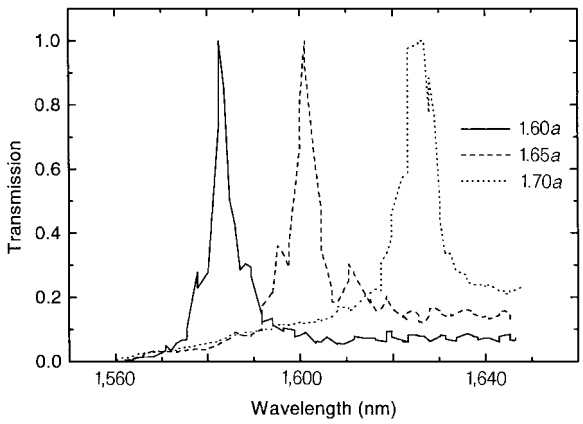

Figure 4 Transmission characteristic of PBG waveguide microcavities for various defect lengths. Three different defect lengths are shown. The resonance peak shifts to longer wavelengths with increasing defect length.

for defects ranging in length from 1.60a to 1.70a. Two phenomena are evident. As the defect length increases, the resonance wavelength shifts to longer values, and the cavity Q is reduced. The increase in cavity length results in a corresponding increase in the effective index 'seen' by the resonant mode, reducing the frequency of the mode. This reduction enhances the coupling of the resonant mode to the waveguide mode, which, in turn, increases the cycle-average radiation out of the cavity and hence reduces the Q.

To study the PBG microcavities, we concurrently developed submicrometre optical waveguides[9]. The reduction in size achieved with high-dielectric contrast materials (these waveguides have cross-sectional dimensions more than an order of magnitude smaller than common low-index-difference waveguides) can lead to densely integrated waveguide structures for optical communication systems. This waveguide technology could lead to an integrated optics approach compatible in materials and dimensions with integrated electronics.

The experimental verification of PBG theory presented above provides confidence that this technology is realizable at optical communication frequencies and can pave the way to the development of novel devices. Because of its high Q/V ratio, the PBG waveguide microcavity can be considered for use in spontaneous-emission-enhancement devices, such a resonant-cavity light-emitting diodes. The control of spontaneous emission is of interest for increasing the light output and narrowing the linewidth of light-emitting diode structures, and for reducing the lasing threshold of semiconductor lasers. By coupling an optical transition to the microcavity resonance, the spontaneous emission rate can be enhanced by a factor η over the rate with no cavity. The expression for η is given as[10]

$$\eta = \frac{Q}{4\pi V}\left(\frac{c}{n\nu}\right)^3 \qquad (2)$$

where c is the speed of light and ν is the optical transition frequency. For the specific PBG waveguide microcavity shown in Fig. 2, this enhancement factor is calculated to be 35, which is significantly larger than any enhancement yet measured. This large spontaneous-emission enhancement could lead to the development of zero-threshold laser devices and efficient erbium-doped Si light emitters. An additional advantage of the PBG waveguide microcavity over more conventional stacked mirror microcavities is the large band-gap. With a 400 nm stop-band, it is possible to have only a single resonant mode in the gain bandwidth of a semiconductor device. The single-mode resonance reduces the available pathways for optical emission away from the resonant wavelength, and channels all of the available optical power into the resonant mode. In contrast with vertically integrated resonant-cavity devices, the configuration used here allows a light-emitting cavity to be directly coupled into a waveguide, so that light collection from the cavity is highly efficient. □

Received 23 July; accepted 23 September 1997.

1. Joannopoulos, J. D., Villeneuve, P. R. & Fan, S. Photonic crystals: putting a new twist on light. *Nature* **386,** 143–149 (1997).
2. Soukoulis, C. M. (ed.) *Photonic Band Gap Materials* (Kluwer, Dordrecht, 1996).
3. Joannopoulos, J. D., Meade, R. D. & Winn, J. N. *Photonic Crystals* (Princeton, New York, 1995).
4. Yablonovitch, E. Photonic band-gap structures. *J. Opt. Soc. Am. B* **10,** 283–295 (1993).
5. Kraus, T., De La Rue, R. & Band, S. Two-dimensional photonic bandgap structures operating at near-infrared wavelengths. *Nature* **383,** 699–702 (1996).
6. Grüning, U., Lehmann, V., Ottow, S. & Busch, K. Macroporous silicon with a complete two-dimensional photonic bandgap centered at 5 μm. *Appl. Phys. Lett.* **68,** 747–749 (1996).
7. Fan, S., Winn, J. N., Devenyi, A., Chen, J. C., Meade, R. D. & Joannopoulos, J. D. Guided and defect modes in periodic dielectric waveguides. *J. Opt. Soc. Am. B* **12,** 1267–1272 (1995).
8. Yang, I. Y. *et al.* Combining and matching optical, e-beam and x-ray lithographies in the fabrication of Si CMOS circuits with 0.1 and sub-0.1 μm features. *J. Vacuum Sci. Technol. B* **13,** 2741–2744 (1995).
9. Foresi, J. S. thesis, MIT (1997).
10. Yokoyama, H. & Brorson, S. D. Rate equation analysis of microcavity lasers. *J. Appl. Phys.* **66,** 4801–4805 (1989).

Acknowledgements. This work was supported by the Air Force Office of Scientific Research (AFOSR), the National Science Foundation (NSF-MRSEC) and the Army Research Office (ARO).

Correspondence and requests for materials should be addressed to P.R.V. (e-mail: pville@mit.edu).

Branched fractal patterns in non-equilibrium electrochemical deposition from oscillatory nucleation and growth

Vincent Fleury

Laboratoire de Physique de la Matière Condensée, École Polytechnique, 91128 Palaiseau cedex, France

The branched fractal structures formed by non-equilibrium electrodeposition of metals[1] have for several years been considered as model systems for the study of branching and fractal growth processes generally[2–6]. Most studies have focused on the large-scale structure of the deposits, but the question of how the branching pattern emerges from the nucleation and growth of the polycrystalline metal at the microscopic scale remains unclear. Here I present experimental and theoretical results which suggest that branched electrodeposits may arise from an oscillatory character in the nucleation kinetics. For this kind of deposition, nucleation is probabilistic but biased towards higher electric fields. I suggest that a given nucleation event is followed by a recovery phase before a subsequent event is possible. This oscillatory nature generates a polycrystalline deposit, the grain size of which determines the level of 'noise' which is amplified by the familiar laplacian ('fingering') instabilities of non-equilibrium growth[2–6] into a macroscopically fractal structure.

Fractal models of growth[2–4] assume that single 'grains' of the same size diffuse and aggregate (the so-called diffusion-limited aggregation model[6]) or nucleate probabilistically on the border of the structure (the dielectric breakdown model[7]). However, true polycrystalline fractal structures are made of grains of a given size, which neither diffuse nor have their final radius instantly at nucleation. I now investigate how the grain texture at the small scale of the deposit is connected to the branched structure of the large scale, and to the fields driving the growth. In particular, how does the growth speed of individual grains match the average growth speed of the branched structure at the larger scale? What determines the size of the grains and the formation of new nucleation events?

The experimental method consists of growing branched metallic structures by electrochemical deposition (ECD), and studying them from the scale of individual grains. For this I have used a new type of electrochemical cell. Glass slides are covered with a thin gold coating and used as support for the growth. Two gold edges, 1,000 Å thick, are deposited 2 cm apart on the support. Copper foil is used as spacers on the cathodic and anodic sides. The deposit starts growing from the 1,000 Å gold cathode, and keeps growing on the slide. The deposit remains on the substrate after cell rinsing and can be used for further analyses. The growth was performed in cells of thicknesses 15 μm, 50 μm and 100 μm. Solutions of $CuSO_4$ of concentrations 0.01, 0.02, 0.04 and 0.1 were used. Constant current was applied in the range 1–100 μA. With this set-up, I obtained robust branched deposits which could be observed *in situ* up to a magnification of ×400, and *ex situ* in the scanning electron microscope (SEM) and atomic force microscope (AFM). The growth was recorded on VHS tape with a CCD (charge-coupled device) camera, and analysed with NIH Image software.

The measured growth speed of the deposit in the range of parameters studied is roughly equal to that predicted by Chazalviel's theory[18] (Table 1), which is the recession speed of the anions[8–11] in the bulk. The SEM (Fig. 1) shows that the branches are made of a